Investigation of spectral gain narrowing in quantum cascade lasers using terahertz time domain spectroscopy

N. Jukam,[1] S. S. Dhillon,[1,a)] D. Oustinov,[1] Z.-Y. Zhao,[1] S. Hameau,[1] J. Tignon,[1,b)] S. Barbieri,[2] A. Vasanelli,[2] P. Filloux,[2] C. Sirtori,[2] and X. Marcadet[3]
[1]*Laboratoire Pierre Aigrain, Ecole Normale Supérieure, 75231 Paris Cedex 05, France*
[2]*Matériaux et Phénomènes Quantiques, Université Paris 7, 75251 Paris Cedex 05, France*
[3]*Thales Research and Technology, Domaine de Corbeville, 91404 Orsay Cedex, France*

(Received 17 May 2008; accepted 18 August 2008; published online 12 September 2008)

The spectral gain of bound-to-continuum terahertz quantum cascade lasers (QCLs) is measured as a function of current density using terahertz time-domain spectroscopy. During lasing action the full width at half maximum (FWHM) of the gain is found to monotonically decrease with increasing current density until lasing action stops at which point the FWHM reaches a minimum (0.22 THz for a laser operating at 2.1 THz). Band structure calculations show that the spectral gain narrowing is due to the alignment and misalignment of the injector with the active region as a function of the applied bias field. © *2008 American Institute of Physics*. [DOI: 10.1063/1.2979682]

Important progress on terahertz quantum cascade lasers (QCLs) has been achieved in the last few years leading to long wavelength,[1] high power,[2] low current,[3] and high temperature operation.[4] In order to realize further improvements, a better understanding of the gain formation mechanism and its limiting factors is needed. To this end it is necessary to perform detailed measurements of the gain including its spectral shape. Previous gain studies for mid-infrared QCLs have used electroluminescence and a coupled cavity scheme.[5] However, in the THz regime such electroluminescence based studies are difficult because of the reduced spontaneous emission at longer wavelengths. Multiple probe pulses coupled into the QCL's end facets can also be used to investigate the temporal dynamics of the gain. Coherent population transfer and gain saturation have been observed with this technique in the mid-infrared.[6,7] Recently, terahertz time-domain spectroscopy (TDS) has been shown to be a powerful technique to measure the gain spectra in QCLs.[8,9] Here, a broadband terahertz probe pulse is coupled into the QCL, and the gain is determined from the electric field of the transmitted pulses.

In this letter terahertz TDS is used to investigate the linewidth of the spectral gain as a function of current density. Two terahertz QCL lasers with different bound-to-continuum designs are studied, one operating at 2.1 THz (Ref. 10) and the other at 2.9 THz (Ref. 11). We observe a decrease in the full width at half maximum (FWHM) of the gain as the current density is increased from threshold. After the laser reaches maximum power, this gain narrowing increases sharply until laser action ceases. By calculating the band structure for different bias fields, we show that the gain narrowing is a consequence of a misalignment of the upper state of the laser transition with the injector miniband.

The 2.1 THz (2.9 THz) sample has an active region thickness of 14 μm (12 μm), and a ridge width of 230 μm (212 μm). Details on the design, processing, and performance can be found elsewhere.[10,11] Samples were cleaved into 3 mm long laser bar and bonded with indium to Au-coated copper holders, which are then mounted onto a cold finger of a continuous flow helium cryostat.

The terahertz probe pulses are generated using a mode-locked femtosecond Ti:sapphire laser and a photoconductive antenna.[12] The terahertz pulses are then collimated and refocused with parabolic mirrors onto the facet of the QCLs in the cryostat. After passing through the QCLs, the transmitted terahertz probe pulses are detected using free space electro-optic sampling (200 μm ZnTe crystal).[9]

A great advantage of this technique is that the phase of the emitted QCL radiation is not locked in time with respect to the femtosecond probe beam; therefore, no electro-optic signal is detected from the QCL emission, allowing spectral investigations below and above laser threshold. This would not be possible with an intensity-based detection technique since the QCL emission incident on the detector would be several orders of magnitude greater than the terahertz probe pulses.

The QCL is modulated with 10 μs electrical pulses with a period of 40 μs. The antenna is modulated with 10 μs electrical pulses with a period of 20 μs such that the QCL was on and then off for every other antenna pulse. The gain spectra can then be derived using the difference field (QCL on and off) and a reference field.[9] The terahertz field coupled into the device is less than 10 V/cm, much less than the internal fields of the QCL.

Figure 1(a) shows the transmitted difference field for various current densities for the 2.1 THz QCL. Oscillations of the electric field are observed, that are due to the amplification of the input pulse at the QCL gain. [Very few field oscillations are observed for low current densities (30 A/cm^2)]. At the threshold current (J_{th}=89 A/cm^2) the field oscillations die out quickly. As the current density (and hence the bias field) is increased more and longer lasting oscillations are observed. At the laser shutoff current (136 A/cm^2), the field oscillations last almost twice as long as at threshold, indicating a reduction in the spectral width. The gain spectra of the 2.1 THz device are shown in Fig. 1(b), clearly showing peak gain at 2.1 THz. As the applied bias is increased the linewidth of the main peak at 2.1 THz decreases. This can also be seen in the inset of Fig. 1(b),

a)Electronic mail: sukhdeep.dhillon@lpa.ens.fr.
b)Electronic mail: jerome.tignon@lpa.ens.fr.

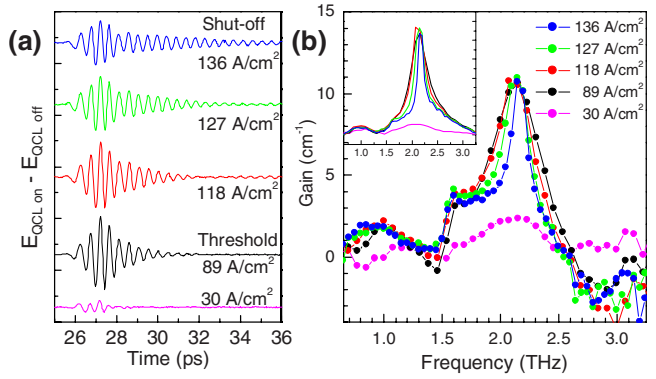

FIG. 1. (Color online) (a) Difference electric fields ($E_{\mathrm{QCL\ ON}}-E_{\mathrm{QCL\ OFF}}$) of the 2.1 THz QCL for various current densities. 89 $\mathrm{A/cm^2}$ and 136 $\mathrm{A/cm^2}$ correspond to the laser threshold and the laser shut-off point. (b) Measured spectral gain of the 2.1 THz QCL for various current densities. The insert shows the Fourier transform of the difference fields of (a).

which shows the Fourier transform of the difference field. Besides the main peak at 2.1 THz, a shoulder near 1.6–1.7 THz is present, which appears to be an artifact of a small dip in the reference pulse near 1.6 THz. A broad absorption feature for frequencies greater then 2.5 THz is also present.

Figure 2(a) shows the *V-I* and *L-I* curves of the 2.1 THz laser. Figure 2(b) shows the gain at the laser frequency and the FWHM of the gain as a function of current density. Below threshold the gain of the laser increases sharply after 60 $\mathrm{A/cm^2}$ as the structure begins to align. The measured gain clamps near threshold (93 $\mathrm{A/cm^2}$) at 11 $\mathrm{cm^{-1}}$ due to laser action. The gain remains constant until approximately 136 $\mathrm{A/cm^2}$ (where laser action ceases), after which it decreases rapidly. A point to note is that the voltage does not clamp in these devices, even when taking into account the contact resistance, as the population of the excited laser state is not fixed.[13]

Regarding the FWHM, as the band structure aligns after 60 $\mathrm{A/cm^2}$ the linewidth of the spectral gain decreases as the gain rapidly increases. Near laser threshold there appears to be a discontinuity in the derivative of FWHM with respect to

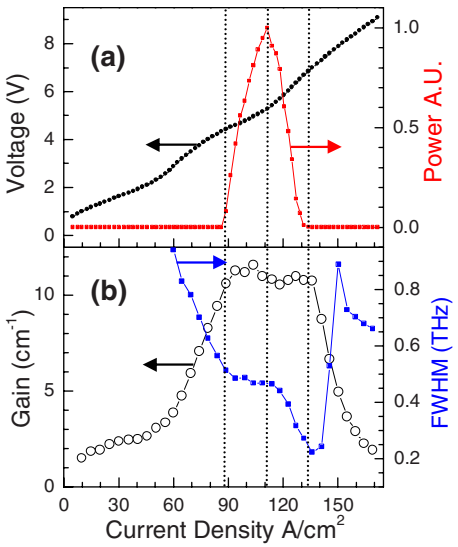

FIG. 2. (Color online) (a) *V-I* and *L-I* curves of the 2.1 THz laser at 4.2K. (b) Spectral gain at the laser frequency and FWHM of the gain as a function of the current density at 4.2 K. The vertical dashed lines correspond to, from left to right, laser threshold, peak power output, and laser shutoff.

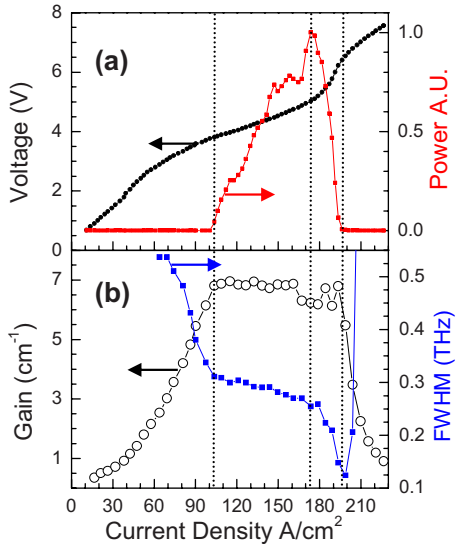

FIG. 3. (Color online) (a) The *V-I* and *L-I* curves of the 2.9 THz laser at 10K. (b) Spectral gain at the laser frequency and FWHM of the gain as a function of the current density at 10 K. The vertical dashed lines correspond to, from left to right, laser threshold, peak power output, and laser shutoff.

current density (dFWHM/dJ) as gain clamping begins. Beyond this point the FWHM decreases at a much slower rate until the laser power saturates at 114 $\mathrm{A/cm^2}$. As soon as the power begins to decrease, a much sharper decrease in the FWHM is observed until it reaches a minimium of 0.22 THz at the shutoff current density of the QCL (136 $\mathrm{A/cm^2}$).

Figure 3 shows *V-I* and *L-I* curves of the 2.9 THz laser along with the maximum spectral gain, the gain at the lasing frequency, and the FWHM of the spectral gain. As in the case of the 2.1 THz laser, before threshold the gain increases and the linewidth decreases until the gain clamps near threshold (104 $\mathrm{A/cm^2}$) at 7 $\mathrm{cm^{-1}}$. At which point the derivative of the FWHM with respect to current density (dFWHM/dJ) undergoes a discontinuity as seen above. After maximum output power (174 $\mathrm{A/cm^2}$), the FWHM decreases at a much greater rate with current density until a minimum linewidth of 0.12 THz is reached at the laser shutoff current of 199 $\mathrm{A/cm^2}$.

For both the 2.1 and 2.9 THz QCLs the spectral gain width narrows during lasing action and decreases dramatically after peak power emission. We qualitatively explain these results in terms of the alignment and misalignment of the wave functions with applied bias. Figures 4(a)–4(c) show the band structure of the 2.1 THz structure for bias fields of 1.5, 1.9, and 2.3 kV/cm, respectively, along with their corresponding moduli squared wave functions. The upper laser states (labeled L1, L2, and L) are red and the miniband states are blue. The active region (where the bulk of the lasing transition's wave functions overlap) consists of three wells separated by two thin barriers. It is indicated by the horizontal arrows in Figs. 4(a)–4(c). The injector miniband states are coupled to the upper laser state via a 50 nm injector well—the pink shaded region in Figs. 4(a)–4(c). The injector state in green (labeled i in Figs. 4(a)–4(c) is mainly confined to this 50 nm injector well. A simplified schematic of the band structures [in Figs. 4(d)–4(f)] indicates the position of the upper laser state with respect to the injector miniband for each of the band structures in Figs. 4(a)–4(c).

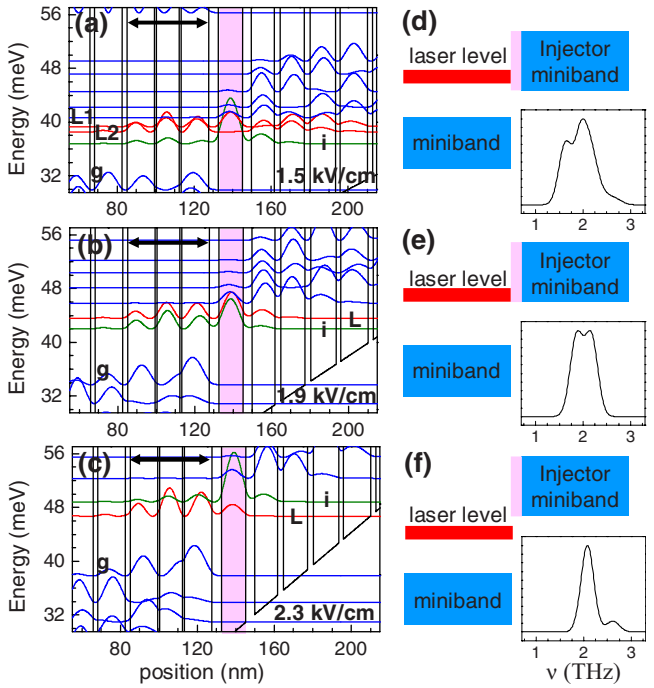

FIG. 4. (Color online) [(a)–(c)] Square modulus of the wave functions with the injector well (shaded pink) for biases of 1.5, 1.9, and 2.3 kV/cm. The upper laser states (red) are labeled L1, L2, and L. The lower laser state is labeled g. The miniband states are in blue. The injector well state (labeled i) is in green. (d)–(f) Schematic of upper laser state and injector miniband alignment corresponding to (a), (b), and (c), respectively. Insets of (d)–(f) show the calculated gain spectra (with a phenomenological broadening parameter).

For low bias fields the upper laser state is aligned with the lower region of the injector miniband as shown in Figs. 4(a) and 4(d) for a field of 1.5 kV/cm. The laser state strongly couples to the closest miniband state, which forms two strongly coupled states [L1 and L2 in Fig. 4(a)] in the active region. The injector state (labeled i) is below levels L1 and L2 in Fig. 4(a), and is weakly coupled to them, indicating nonoptimal injection efficiency.

As the applied bias is increased the injector miniband is shifted to higher energies with respect to the upper laser states. For some bias, the laser state will be aligned with the lowest energy state of the injector miniband (the injector state) as shown in Fig. 4(e). In Fig. 4(b) at a bias field of 1.9 kV/cm, the laser state is strongly coupled to the injector state.[14] Indeed it is difficult to distinguish between the injector and laser states in Fig. 4(b). The strong coupling between the laser and injector states corresponds to resonant current injection[13] into the upper laser level (i.e., the fastest pumping rate) and the maximum emitted power from the QCL.

For bias fields greater than the optimum bias, the injector miniband moves above the upper laser state as shown in Fig. 4(f). This results in a misalignment in the structure, a decrease in the injection efficiency, and hence a drop in the emitted QCL power. This is shown in Fig. 4(c) for a field of 2.3 kV/cm, where the laser state is below the injector state, and the injector and laser states have become uncoupled. Indeed, the oscillator strength between the injector and the lower laser state [labeled g in Figs. 4(a)–4(c)] decreases from a maximum of 10 at a field of 1.9 kV/cm to less than 3 at 2.3 kV/cm. The oscillator strength between the upper and lower laser states changes from 17 at 1.9 kV/cm to 24 at 2.3 kV/cm. Thus for bias fields higher than the optimal injection [i.e., after 1.9 kV/cm, shown in Fig. 4(b)] a *single* upper laser state contributes to the gain.

Therefore, the observed narrowing of the spectral gain width after maximum power is attributed to the formation of single upper laser level. This is in contrast to lower biases, where several highly coupled levels will contribute to the lasing transition. The energy splitting between the strongly coupled levels will increase the width of spectral gain vis-a-vis a single upper laser state. Indeed using a broadening of the gain spectra (0.3 THz) and the dipole moments of each transition, the expected gain spectra are shown in the insets of Figs. 4(d)–4(f) showing gain narrowing as the field is increased. Band structure simulations of the 2.9 THz QCL show a similar effect.

The broad absorption beyond 2.5 THz for the 2.1 THz QCL [Fig. 1(b)] could be due to transitions from the upper lasing states to the first excited miniband levels (not shown in Fig. 4). These features are, however, at the limit of our measuring technique, which only has a spectral response to ~3.3 THz.

In conclusion, narrowing of the gain spectrum with increasing current density has been observed above laser threshold in 2.1 and 2.9 THz bound-to-continuum QCLs using terahertz TDS. The narrowing of the gain spectra is explained in terms of the coupling between the upper laser state and states in the injector miniband. These investigations should have an impact on future QCL designs as well as an increased understanding of the injector-laser state coupling.

This work was financially supported by the DGA, CNano and ANR. The LPA-ENS is a "Unité Mixte de Recherche Associée au CNRS UMR8551 et aux Universités Paris 6 et 7."

[1]C. Walther, M. Fischer, G. Scalari, R. Terazzi, N. Hoyler, and J. Faist, Appl. Phys. Lett. **91**, 131122 (2007).
[2]B. S. Williams, S. Kumar, Q. Hu, and J. L. Reno, Electron. Lett. **42**, 89 (2006).
[3]S. Dhillon, J. Alton, S. Barbieri, C. Sirtori, A. de Rossi, M. Calligaro, H. E. Beere, and D. Ritchie, Appl. Phys. Lett. **87**, 071107 (2005).
[4]M. A. Belkin, J. A. Fan, S. Hormoz, F. Capasso, S. P. Khanna, M. Lachab, A. G. Davies, and E. H. Linfield, Opt. Express **16**, 3242 (2008); B. S. Williams, S. Kumar, Q. Hu, and J. L. Reno, *ibid.* **13**, 3331 (2005).
[5]S. Barbieri, C. Sirtori, H. Page, M. Beck, J. Faist, and J. Nagle, IEEE J. Quantum Electron. **36**, 736 (2000).
[6]F. Eickemeyer, K. Reimann, M. Woerner, T. Elsaesser, S. Barbieri, C. Sirtori, G. Strasser, T. Muller, R. Bratschixch, and K. Unterrainer, Phys. Rev. Lett. **89**, 047402 (2002).
[7]H. Choi, T. B. Norris, T. Gresch, M. Girovannini, J. Faist, L. Diehl, and F. Capasso, Appl. Phys. Lett. **92**, 122114 (2008).
[8]J. Kröll, J. Darmo, S. S. Dhillon, X. Marcadet, M. Calligaro, C. Sirtori, and K. Unterrainer, Nature (London) **449**, 698 (2007).
[9]N. Jukam, S. S. Dhillon, Z. Y. Zhao, G. Duerr, J. Armijo, N. Sirmons, S. Hameau, S. Barbieri, P. Filloux, C. Sirtori, X. Marcadet, and J. Tignon, IEEE J. Sel. Top. Quantum Electron. **14**, 436 (2008).
[10]C. Worrall, J. Alton, M. Houghton, S. Barbieri, H. E. Beere, D. A. Ritchie, and C. Sirtori, Opt. Express **14**, 171 (2006).
[11]S. Barbieri, J. Alton, H. E. Beere, J. Fowler, E. H. Linfield, and D. A. Ritchie, Appl. Phys. Lett. **85**, 1674 (2004).
[12]A. Dreyhaupt, S. Winnerl, T. Dekorsy, and M. Helm, Appl. Phys. Lett. **86**, 121114 (2005).
[13]C. Sirtori, F. Capasso, J. Faist, A. L. Hutchinson, D. L. Sivco, and A. Y. Cho, IEEE J. Quantum Electron. **34**, 1722 (1998).
[14]The energy splitting between the upper laser state and the injector state is a local minimum at 1.9kV/cm which indicates that maximium coupling between the states.